Polymorphism in $Ho_2(MoO_4)_3$

C. González-Silgo,[1,a)] C. Guzmán-Afonso,[2] V. M. Sánchez-Fajardo,[3] S. Acosta-Gutiérrez,[1] A. Sánchez-Soares,[1] M. E. Torres,[3] N. Sabalisck,[3] E. Matesanz,[4] and J. Rodríguez-Carvajal[5]
[1]*Dpto. Física Fundamental II, Universidad de La Laguna, Avda. Astrofísico Fco. Sánchez, s/n, 38206 La Laguna, Tenerife, Spain*
[2]*Dpto. Física Fundamental y Experimental, Electrónica y Sistemas, Universidad de La Laguna, Avda. Astrofísico Fco. Sánchez, s/n, 38206 La Laguna, Tenerife, Spain*
[3]*Dpto. Física Básica, Universidad de La Laguna, Avda. Astrofísico Fco. Sánchez, s/n, 38206 La Laguna, Tenerife, Spain*
[4]*C.A.I. Difracción de Rayos X, Universidad Complutense de Madrid, 28040 Madrid, Spain*
[5]*Institut Laue-Langevin, 6 rue Jules Horowitz, BP 156, 38042 Grenoble Cedex 9, France*

[a)]Electronic mail: csilgo@ull.es

Two polymorphs of Holmium molybdate, known as *β'*-phase and *γ*-phase, were prepared by solid state reaction with different thermal treatments. These polycrystalline samples have been studied for the first time by X-ray thermodiffractometry from room temperature up to 1300 K. We found that the initial *β'*-phase undergoes a transition to a-*β*-phase and then to a *γ*-phase. The *γ* (hydrated)-phase, turns to the *γ* (dehydrated)-phase and then to the *β*-phase. Each sequence involves a reversible and an irreversible phase transition for $Ho_2(MoO_4)_3$. Both polymorphs have remarkable physical properties like nonlinear optics, ferroelectricity and negative thermal expansion. We have calculated the linear expansion coefficients of both phases. We have obtained a positive coefficient for the *β'*-phase and a negative one for the *γ*-phase. Moreover, we have made a comparison of the obtained coefficients with previous results for other rare earth molybdates.

Key words: powder diffraction, phase transition, polymorphism

I. INTRODUCTION

All the known structures of molybdates at room temperature, with general composition noted as $RE_2(MoO_4)_3$ (RE=rare earth) and depending on the ionic radius, belong to four structure types: $La_2(MoO_4)_3$ (Jeitschko, 1973), $Eu_2(WO_4)_3$ (Templeton and Zalkin, 1963), *β'*-

https://doi.org/10.1017/S0885715613001176 Published online by Cambridge University Press

$Gd_2(MoO_4)_3$ (Jeitschko, 1972) and $Sc_2(WO_4)_3$ (Abrahams and Bernstein, 1966). Rare earth molybdates with intermediate ionic radii show the β'-$Gd_2(MoO_4)_3$ ferroelectric-ferroelastic phase. The $Gd_2(MoO_4)_3$, with *Pba*2 space group attracts attention since it has shown to be an efficient frequency doubling medium for laser diode pumping (Kojima and Nakamura, 1978). The corresponding paraelectric-paraelastic phase (β) belongs to the P-42_1m space group and arises after a phase transition at about 450 K. The heavier molybdates with the $Sc_2(WO_4)_3$ structure type have a *Pbcn* space group; this structure is known as γ-phase and exhibits negative thermal expansion (NTE) (Guzmán-Afonso *et al.*, 2011). A possible ferroelastic phase (γ'-phase), with positive thermal expansion, is expected at very low temperatures but it has only been found in some isostructural compounds (Evans and Mary, 2000).

Holmium trimolybdate belongs to the family of rare earth trimolybdates, with two stable phases at room temperature: γ (hydrated) and β'. The coexistence of these two phases has only been studied in $Y_2(MoO_4)_3$ at room temperature (Gates and Lind). In this work we will study the sequence of reversible and irreversible phase transitions of the two $Ho_2(MoO_4)_3$ phases that appear while increasing the temperature.

II. EXPERIMENTAL

A. Synthesis

Polycrystalline holmium trimolybdates were prepared by conventional solid-state synthesis (Kim *et al.*, 1991). We have obtained the initial β' and γ (hydrated) phases by using different thermal treatments: 1173 K for 24 h and 1250 K for 48 h, respectively. We will name them with their "initial phase" in the following X-ray experiments discussion.

B. X-ray diffraction

X-ray thermodiffractometry was performed using a PANalytical X'Pert PRO diffractometer with Bragg-Brentano geometry and Cu $K\alpha$ radiation (45 KV and 40 mA). An

https://doi.org/10.1017/S0885715613001176 Published online by Cambridge University Press

X'Celerator detector was employed to collect XRD data over the 2θ angular range from 5° to 80° with a step size of 0.017° and a counting time of 50 and 100 s/step for the γ and β' phases, respectively. The samples were measured at different temperature ranges: from 300 K to 1000 K (in steps of 25 K) for the initial γ-$Ho_2(MoO_4)_3$ phase; and from 300 K to 1300 K (in steps of 20 K) for the initial β'-$Ho_2(MoO_4)_3$ phase. Measurements were carried out during a heating process under a still air atmosphere using an Anton Paar HTK 2000 camera.

III. RESULTS AND DISCUSSION

We have plotted the diffraction patterns measured for each sample using the 2D Contour tool of the FullProf software (Rodríguez-Carvajal, 1993). Figure 1 shows the sequence of phase transitions for $Ho_2(MoO_4)_3$ in the studied temperature range. We found that the initial β'-phase undergoes a transition to the β-phase (reversible process) and then to the γ-phase (irreversible process), which becomes hydrated at room temperature. For the other polymorph, the initial hydrated γ-phase turns to γ-phase (reversible process) and then to the β-phase (irreversible process), which changes to the β'-phase at room temperature.

The first transition of the (initially) β'-$Ho_2(MoO_4)_3$ sample occurs at 400 K and the second transition between 1125 and 1200 K. For the (initially) γ (hydrated)-$Ho_2(MoO_4)_3$ sample, the first transition takes place around 400 K and the second one between 780 and 920 K. The second transition of each sample occurs within a temperature interval in which the β and γ phases coexist. It can be seen that the transformation from the γ-$Ho_2(MoO_4)_3$ to the β-$Ho_2(MoO_4)_3$ is slower than the reverse process.

https://doi.org/10.1017/S0885715613001176 Published online by Cambridge University Press

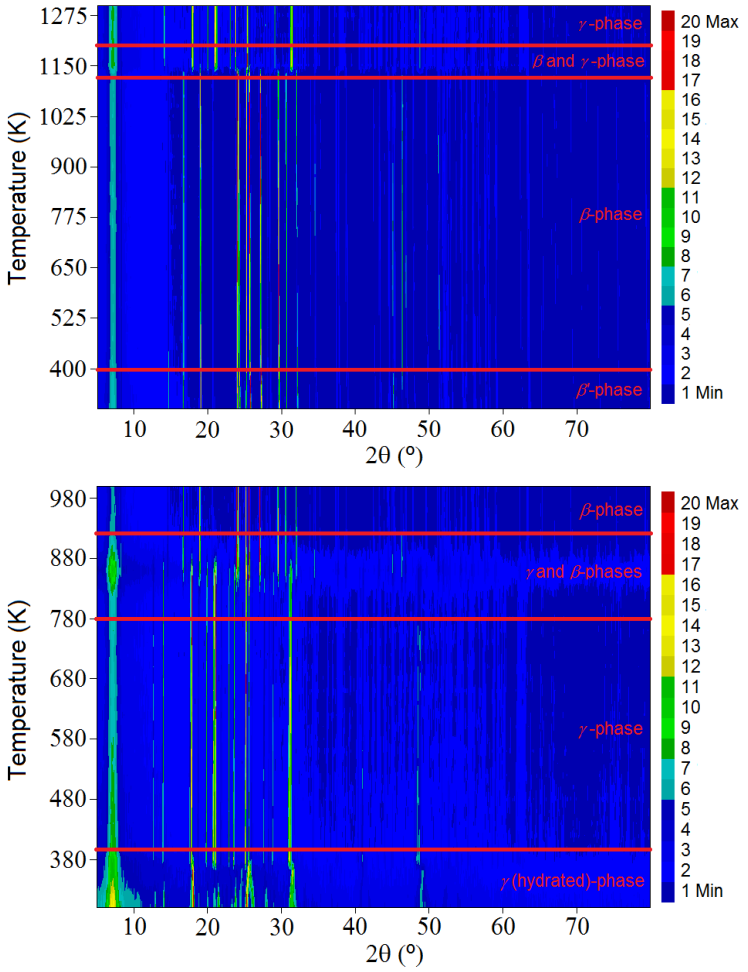


Figure 1. 2D contour plot of the X-ray diffraction patterns for the initial β'-phase (up) and for the γ (hydrated)-phase (down). Each pattern has been normalized to the highest peak. The red lines divide the temperature range into regions with different structural phases.

In order to obtain the thermal dependence of the crystallographic cell parameters, we have analyzed the X-ray diffraction patterns. We have obtained the scale factor, instrument zero, cell parameters, microstrain and domain size (given by U and Y parameters from the Thompson-Cox-Hasting pseudo-Voigt profile shape function) and the background coefficients (modeled by a Chebyshev polynomial) from powder diffraction data by iterating full pattern profile fittings [with the Le Bail (2005) algorithm] using the FullProf software (Rodríguez-Carvajal, 1993). We have used the sequential mode to perform the profile matching of all diffractograms. This method is useful when the processing of a large number of diffraction patterns that have been collected during a single experiment as function of an external parameter is desired, and the changes between two consecutive patterns are very small. The results of the refinements provided the reliability factors, χ^2, R_B, and R_{wp}, varying from 1.5 to 2.4, 0.7 to 1.8% and from 0.3

https://doi.org/10.1017/S0885715613001176 Published online by Cambridge University Press

to 2.3%, respectively. The patterns from 300 to 400 K for γ (hydrated)-$Ho_2(MoO_4)_3$ were not fitted. Figure 2 shows two examples of obtained profile matching using the described procedure in this work. Both diffraction patterns belong to the initial samples, phases β' and γ (hydrated), measured after heating to 1000 K and had already transformed into the β-phase. The diffractograms are very similar, so that the Bragg positions appear at the same angles and the relative intensities are equal. We were not able to compare the γ-phase, since we did not heat the initial γ-phase beyond 1200 K, where we would expect a β-γ phase transition, according to the synthesis conditions and the phase relationships of the $RE_2(MoO_4)_3$-type rare earth molybdates, given by Brixner *et al.*, (1979). The γ-β phase transition was not described by the mentioned authors.

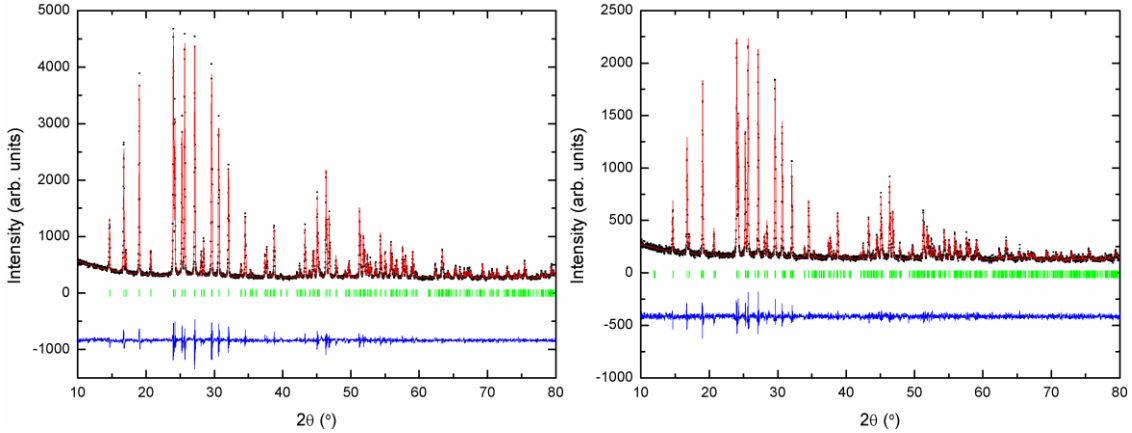


Figure 2. Profile matching for the initial β'-phase sample (left) and for the initial γ (hydrated)-phase sample (right) at 1000 K. Both patterns were indexed with the β-phase. The dotted line indicates observed intensities, and the profile fit is shown by a red line. The difference between observed and calculated intensities is plotted with a blue line, and the vertical bars represent the expected positions of diffraction peaks.

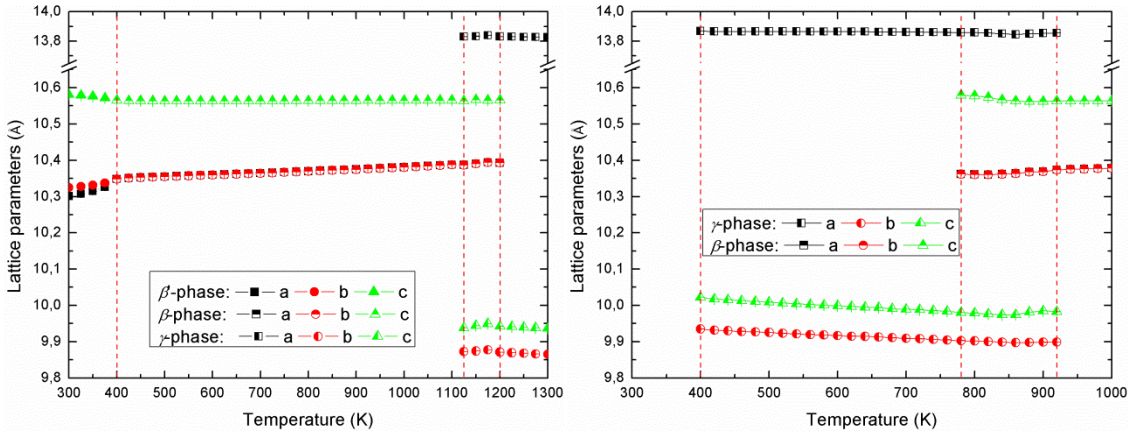


Figure 3. Temperature dependence of the lattice parameters for the initial β'- $Ho_2(MoO_4)_3$ (left) and for the γ-$Ho_2(MoO_4)_3$ (right). The red dashed lines divide the temperature range into regions with different structural phases.

https://doi.org/10.1017/S0885715613001176 Published online by Cambridge University Press

Figure 3 shows the variation of the unit-cell structural parameters for the initial samples: *β'* and *γ*-$Ho_2(MoO_4)_3$. On the left figure we have the lattice parameters of the initial *β'*-phase and their thermal dependence. For this sample, the **a** and **b** parameters increase when the temperature increases and become equal at completion of the transformation into the *β* phase. The **c** parameter decreases until the transformation into the *β* phase, and then it continues decreasing more slowly until it reaches the *γ* phase, when all the cell parameters decrease. The thermal dependence of cell parameters for the sample with an initial *γ*-phase can be seen in figure 3 (right). At first all the cell parameters decrease with increasing temperature; when the phase transition to the *β* phase has been completed, the **a** and **b** parameters increase slightly with temperature, while the **c** parameter remains constant. During the coexistence of both phases there is an anomalous behavior: the slopes of the thermal dependence of the cell parameters change.

Figure 4 shows the thermal dependence of volume for both samples. The more dense *β'*-phase expands when the temperature increases, but it shows an anomalous behavior during the coexistence of phases. The behavior around the ferroelectric-paraelectric phase transition is similar to other molybdates: $LaEr(MoO_4)_3$, $Tb_2(MoO_4)_3$ and $Dy_2(MoO_4)_3$, which we have studied from 225 to 375 K (González-Silgo *et. al.*, 2011). The obtained coefficient for for *β'*-$Ho_2(MoO_4)_3$ was 1.02×10^{-5} K^{-1}, in this temperature interval. At higher temperatures, we have observed a similar dependence to other trimolybdates (González-Silgo *et. al.*, 2011). On the other hand, we have found that the less dense sample *γ* (dehydrated)-$Ho_2(MoO_4)_3$ exhibits negative thermal expansion from 400 to 780 K, after water loss, as it is observed with other similar molybdates (Guzmán-Afonso *et al.*, 2011) and from 1125 K to melting. We have calculated the linear thermal expansion coefficient α_L (negative value) until 780K for γ-$Ho_2(MoO_4)_3$, and we have confirmed that α_L is less negative when the ionic radius decreases (Guzmán-Afonso *et al.*, 2011). The calculated value was -6.25×10^{-6} K^{-1}; thus, it shows the largest negative linear expansion coefficient for this family of compounds. When both phases coexist, the behavior is anomalous and it is correlated with the *β* phase. During the *β*-*γ* phase transition, their volume increases just before the disappearance of the phase *β*; whereas during the *γ*-*β* phase transition, the volume of both phases decrease and its thermal dependence turns positive before the disappearance of the phase *γ*. After this, the volume of the *β* phase increases normally.

https://doi.org/10.1017/S0885715613001176 Published online by Cambridge University Press

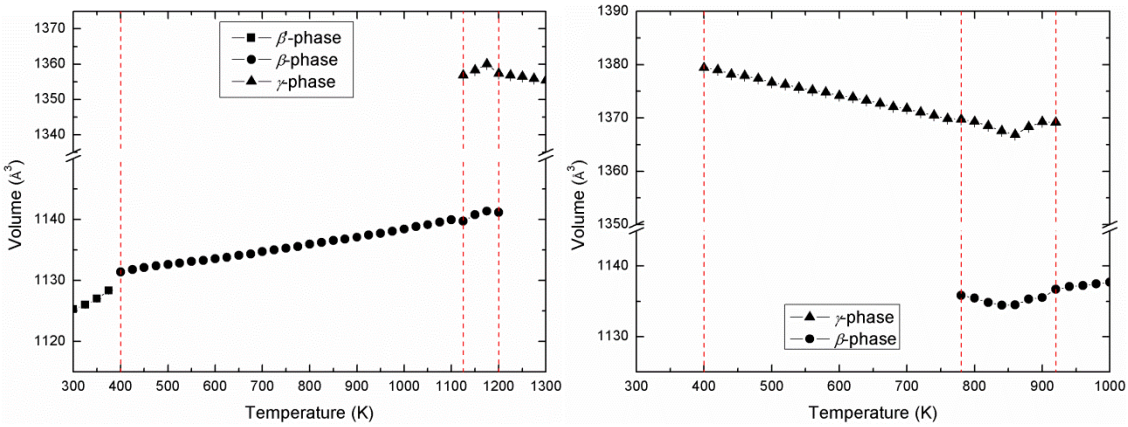


Figure 4. Temperature dependence of volume for the initial *β'*-phase sample (left) and for the *γ*-phase sample (right). The red dashed lines divide the temperature range into regions with different structural phases.

IV. **CONCLUSION**

Holmium molybdate can crystallize in two different phases (*β'* and *γ)* and their structural parameters are known at room temperature. We have described the evolution of both phases with the temperature. We have obtained a different phase diagram depending on the starting phase. We have analyzed the evolution of the lattice parameters and the volume of both samples. Two reversible phase transitions: *β'*-*β* and *γ* (hydrated) - *γ* (dehydrated) and two irreversible phase transitions *β*-*γ* and *γ*-*β* (with the latter exhibiting phase coexistence) have been detected for each starting sample. The *β'*-*β* phase transition is similar to other studied compounds*:* when the ionic radius decreases, the positive linear expansion coefficient is positive, although the **c** parameter decreases when the temperature increases (González-Silgo *et. al.*, 2011). Negative thermal expansion has been found for the *γ*-phase, and the negative linear expansion coefficient decreases when the ionic radius decreases, as observed for similar compounds (Guzmán-Afonso *et al.*, 2011). However, an anomalous behavior has been detected during the coexistence of phases. This last result could help us understand the negative expansion. Therefore we need to study the crystal structure of both phases during the irreversible phase transition. The ILL research proposal number 57431 has been accepted to perform a neutron diffraction experiment in the D2B beamline at high temperature, starting from the *γ* phases of $Ho_2(MoO_4)_3$, $Ho_2(WO_4)_3$, $Tm_2(MoO_4)_3$ and $Tm_2(WO_4)_3$.

https://doi.org/10.1017/S0885715613001176 Published online by Cambridge University Press

ACKNOWLEDGMENTS

The authors are grateful to the Ministerio de Ciencia e Innovación of Spain (MICCIN) under The National Program of Materials (MAT2010-21270-C04-02), the Consolider-Ingenio 2010 Program (MALTA CSD2007-0045), and to EU-FEDER funds for their financial support. C. Guzmán-Afonso wishes to thank ACIISI and FSE for a fellowship.

Abrahams, S. C. and Bernstein, J. L. (**1966**). "Crystal Structure of the Transition-Metal Molybdates and Tungstates. II. Diamagnetic $Sc_2(WO_4)_3$," J. Chem. Phys. **45**, 2745-2752.

Brixner, L. H., Barkley, J. R. and Jeitschko, W. (**1979**). *Handbook on the Physics and Chemistry of Rare Earth* (Amsterdam: North-Holland).

Evans, J. S. O and Mary, T. A. (**2000**). "Structural phase transitions and negative thermal expansion in $Sc_2(MoO_4)_3$," Int. J. Inorg. Mater. **2**, 143-151.

Gates, S. D. and Lind, C. (**2007**). "Polymorphism in yttrium molybdate $Y_2Mo_3O_{12}$," J. Solid State Chem. **180**, 3510-3514.

González Silgo, C., Torres, M. E., Guzmán-Afonso, C., Sabalisck, N., Lozano-Gorrín, A. D., González-Platas, J., Matesanz, E., Rodríguez-Carvajal. J. (2011). Crystal structure and non-linear properties of A2(MoO4)3 (Report Proposal 5-23-626). Grenoble, France: Institut Laue-Langevin user portal. https://club.ill.fr/cv/servlet/ReportFind

Guzmán-Afonso, C., González-Silgo, C., González-Platas, J., Torres, M. E., Lozano-Gorrín, A. D., Sabalisck, N., Sánchez-Fajardo, V., Campo, J. and Rodríguez-Carvajal, J. (**2011**). "Structural investigation of the negative thermal expansion in yttrium and rare earth molybdates," J. Phys.: Condens. Matter **23**, 325402 (9pp).

Jeitschko, W. (**1973**). "Crystal structure of $La_2(MoO_4)_3$, a new ordered defect Scheelite type," Acta Crystallogr., Sect. B: Struct. Crystallogr. Cryst. Chem. **29**, 2074-2081.

Jeitschko, W. (**1972**). "A Comprehensive X-ray Study of the Ferroelectric-Ferroelastic and Paraeleetric-Paraelastic Phases of $Gd_2(MoO_4)_3$," Acta Crystallogr., Sect. B: Struct. Crystallogr. Cryst. Chem. **28**, 60-76.

Kim, S., Lee, G.S., Shrout, T.R. and Venkataramani, S. (**1991**). "Fabrication of fine-grain piezoelectric ceramics using reactive calcination," J. Mater. Sci. **26**, 4411-4415.

Kojima, S. and Nakamura, T. (**1978**). "Electro-optical properties of gadolinium molybdate," Phys. Rev. B **18**, 453-458.

Le Bail, A. (**2005**). "Whole powder pattern decomposition methods and applications: A retrospection," Powder Diffr. **20**, 316-326.

Rodríguez-Carvajal, J. (**1993**). "Recent advances in magnetic structure determination by neutron powder diffraction," Physica B **192**, 55-69.

Templeton, D. H. and Zalkin, A. (**1963**). "Crystal structure of europium tungstate," Acta Crystallogr. **16**, 762-766.

https://doi.org/10.1017/S0885715613001176 Published online by Cambridge University Press